Combustion and Flame xxx (xxxx) xxx

Contents lists available at ScienceDirect

Combustion and Flame

journal homepage: www.elsevier.com/locate/combustflame

CO assisted NH_3 oxidation

María U. Alzueta[a,*], Iris Salas[a], Hamid Hashemi[b], Peter Glarborg[b]

[a] Aragón Institute of Engineering Research (I3A), Department of Chemical and Environmental Engineering, University of Zaragoza, Zaragoza 50018, Spain
[b] DTU Chemical Engineering, Technical University of Denmark, Lyngby DK-2800, Denmark

ARTICLE INFO

Article history:
Received 4 July 2022
Revised 10 October 2022
Accepted 10 October 2022
Available online xxx

Keywords:
Ammonia
NH_3
Carbon monoxide
CO, NH_3-CO-NO interaction
Nitric oxide
NO

ABSTRACT

In the present work, experimental results from the literature on the effect of CO on the NH_3 oxidation in the absence and presence of NO are supplemented with novel flow reactor results and interpreted in terms of a detailed chemical kinetic model. The kinetic model provides a satisfactory prediction over a wide range of conditions for oxidation in flow reactors and for flame speeds of CO/NH_3. With increasing levels of CO, the generation of chain carriers gradually shifts from being controlled by the amine reaction subset to being dominated by the oxidation chemistry of CO, facilitating reaction at lower temperatures. At elevated temperature, presence of CO causes a change in selectivity of NH_3 oxidation from N_2 to NO. The present work provides a thorough evaluation of the amine subset of the reaction mechanism for the investigated conditions and offers a kinetic model that reliably can be used for post-flame oxidation modeling in engines and gas turbines fueled by ammonia with a hydrocarbon or alcohol as co-fuel.

1. Introduction

Climate change, security of energy supply, and fossil fuels depletion provide an incentive for a transition to a low-carbon economy. Ammonia is a carbon-free fuel and can be a suitable alternative for stationary power, transportation, and energy storage applications. Challenges of using ammonia in engines and gas turbines are investigated extensively [1–3]. There has been a number of studies on the use of NH_3 as an engine fuel, but its poor combustion characteristics for conventional engine combustion techniques have been difficult to overcome. Hence, additional fuels such as hydrogen or carbon-based fuels such as alcohols or diesel fuel have been suggested as combustion promotors. Downstream of the ignition region in engines and gas turbines, ammonia will be oxidized in an environment, which is likely to contain other combustibles, as well as oxygen and nitrogen oxides. Considering that the co-fuel must be more reactive than NH_3 to promote ignition, it can be assumed that CO and H_2 are important intermediates present during the burnout of the ammonia.

To facilitate modeling of the post-flame region, it is of interest to characterize the interaction of CO and H_2 with NH_3. The radical pool generated in the oxidation of CO and/or H_2 will affect the reaction rate and selectivity of the oxidation of NH_3. A large number of studies of oxidation of H_2/NH_3 mixtures have been reported in the literature, including studies of flame behavior [4–15] and ignition delay times [16–19]. Results on oxidation of CO/NH_3 mixtures are more limited, with data available for species concentrations in flow reactor experiments [19–23], flame speeds [8,10], and explosion limits [24].

The presence of NO in the post-flame region will also affect the NH_3 oxidation. The reaction of NH_3 with NO in the presence of O_2 has been studied extensively due to its importance in selective non-catalytic reduction of NO (SNCR) with ammonia [25–27]. Even though the SNCR mechanism is comparatively well understood and the main features of the process can be predicted satisfactorily, quantitative modeling predictions over a wider range of conditions are still elusive [26]. However, the impact of addition of combustibles on SNCR with NH_3 has been studied widely, and results are for addition of both H_2 [20,28–34] and CO [20,22,32–45].

To facilitate the use of ammonia as an energy carrier, it is important to have access to reliable and versatile chemical kinetic models for ignition and oxidation of NH_3. The objective of the present work is to investigate the impact of CO on NH_3 oxidation in the absence and presence of NO. The CO/NH_3 oxidation chemistry is important for the burnout in ammonia-fueled engines and turbines. Furthermore, since the radical pool is partly controlled by the moist CO reaction subset, the results may provide constraints on the amine chemistry that can facilite further development of this reaction subset. Available experimental data in the literature are reviewed, with the most well-defined and reliable results chosen for further analysis. In addition, novel experiments are con-

* Corresponding author.

https://doi.org/10.1016/j.combustflame.2022.112438

ducted in a laminar flow reactor to extend the range of conditions covered in literature. The experimental data are analyzed in terms of a detailed chemical kinetic model. The starting mechanism is drawn from the review by Glarborg et al. [26], but modifications are made according to more recent work.

2. Experimental methodology

Experiments are carried out in an experimental setup that has been used with success in the study of the gas-phase oxidation process of ammonia, among other compounds. A full description of the experimental procedure can be found elsewhere [46–48]. Reactants (NH_3, CO, NO, and O_2, diluted either in argon or nitrogen), are fed from gas cylinders through mass flow controllers and led to a quartz tubular flow reactor in four separate streams, following the procedure of Alzueta et al. [49], and then mixed at the entrance to the reaction zone. The reactor (20 cm length and 0.87 cm inside diameter) is heated electrically by means of a three heating zones oven. At the outlet of the reactor, reaction is quenched by adding air through an external refrigeration jacket. Experiments are made using a total flow rate of 1 L (STP)/min, implying a gas residence time that varies with temperature. At the outlet of the reactor, gases are analyzed using continuous analyzers for NH_3, NO, CO, and CO_2, as well as a gas chromatograph (GC) with TCD detectors for NH_3, H_2, CO, CO_2, O_2, and N_2. The uncertainty of the measurements is estimated to be within 5%, and not less than 5 ppm, for the continuous analyzers, and 10 ppm for the GC [47,48].

The experimental error has been estimated by calculating the pooled standard deviation (the square root of the sum of squares of the error) associated with the NH_3 concentration, following the same procedure as in the work of Colom-Daz et al. [50]. It has been assumed that the experimental error does not depend on the temperature in the range considered. In this way, the pooled standard deviation obtained is 0.05, i.e., 5%. Thus, the uncertainty of the experiments is estimated to be within 5%, and not less than 5 ppm, for the continuous analyzers, and 10 ppm for the GC [47,48].

Since the gases enter the reactor unmixed, the mixing region becomes important at high reaction rates. Kristensen et al. [51] estimated the mixing time in these reactors to be of the order of 5 ms. Their calculations for a reaction system of $CO/NH_3/HCN/NO/O_2$, similar to that of the present work, indicated that depending on the conditions (the inlet CO concentration and the temperature), significant conversion of the reactants may occur within this short time. Thus, at temperatures higher than that of full conversion of CO and NH_3, comparison of modeling predictions with experiment must be interpreted cautiously.

3. Chemical kinetic model

The kinetic model was based on the reaction mechanism of Glarborg et al. [26], drawing on more recent work on amine chemistry by Stagni et al. [52] and by the authors [27,48,53–57]. Important changes include the reactions $NH_2 + HO_2$ [55] and $NH_2 + NO_2$ [57], as well as steps involved in amine pyrolysis [54,56]. The full mechanism is available as Supplementary Material. Table 1 lists selected reactions for chemical coupling between NH_3 and CO, as discussed below.

Under the conditions of interest in this study, CO may be present in high concentrations and recombination reactions involving CO can remove radicals and thereby inhibit reaction. To account for this, subsets for CH_2O (including H + CO (+M) ⇄ HCO (+M)), H_2NCO (including NH_2 + CO (+M) ⇄ H_2NCO (+M)), and HNCO (including NH + CO (+M) ⇄ HNCO (+M)) [26] were included in the mechanism. Only H + CO (+M), followed by HCO + H ⇄ CO + H_2, was found to be important.

Table 1
Selected reactions for chemical coupling between NH_3 and CO. Parameters for use in the modified Arrhenius expression $k = AT^{\beta}\exp(-E/[RT])$. Units are mol, cm, s, cal.

		A	β	E	Source
1.	$H_2NCO(+M) \rightleftarrows CO + NH_2(+M)$	5.9E12	0.000	25,000	[58]
	Low pressure limit	1.0E14	0.00	21,700	
2.	$HNCO + M \rightleftarrows CO + NH + M$	1.1E16	0.000	86,000	[59]
3.	$HOCO + NH_2 \rightleftarrows CO_2 + NH_3$	2.0E13	0.000	0	est
4.	$HOCO + NO \rightleftarrows CO_2 + HNO$	5.0E09	1.000	0	[60], est

Part of the CO may be oxidized through the HOCO intermediate. For this reason, it is relevant to consider reactions of HOCO with reactive nitrogen species. The reaction of HOCO with NO has been studied experimentally [60,61] and theoretically [62] due to its potential importance in the atmosphere. At room temperature, the reaction is slightly faster than HOCO + O_2 [60]; for the rate constant we have relied on the low temperature measurement and assumed that the two reactions have similar temperature dependencies. The main products are HNO + CO_2, with some stabilization of HOC(O)NO at low temperature [61,62]. Also the reaction HOCO + NH_2 ⇄ CO_2 + NH_3 was included with an estimated rate constant. The modeling predictions in the current study were not sensitive to these steps, but they could conceivably become important under the high-pressure conditions in engines and gas turbines.

The rate constants for the reverse reactions were computed from the forward rate constants and the equilibrium constants using the thermodynamic data from the same sources as the kinetic mechanism. Calculations have been performed using the Chemkin-PRO suite of programs [63]. The flow reactor modeling was conducted assuming isothermal conditions unless otherwise stated.

4. Results and discussion

The limited amount of data reported in literature for oxidation of CO/NH_3 mixtures have mostly been obtained in laminar flow reactors. We have selected data from Wargadalam et al. [22] and Kasaoka et al. [20] for analysis in this work, in addition to the results from our own experiments. The studies by Zhao et al. [21], Wang et al. [23], and Chen et al. [19] were disregarded since they employed comparatively high inlet concentrations of CO and O_2. Due to the associated heat release, this introduces an uncertainty in the reaction temperature.

Unlike CO oxidation in the absence of NO, the $CO/NH_3/NO/O_2$ system has been characterized in flow reactor experiments over a fairly wide range of conditions. Here, novel data from the present work at low O_2 levels were supplemented with results from Wargadalam et al. [22], Alzueta et al. [37], and Suhlmann and Rotzoll [35].

Surprisingly, there are no reported studies of the effect of CO on the ignition delay of NH_3 in shock tubes or rapid compression machines. However, flame speed measurements for CO/NH_3 are available [8,10] and they were considered in the present work.

4.1. Effect of CO on NH_3 oxidation in a flow reactor

While the $NH_3/NO/O_2$ system is not sensitive to initiation of reaction [25], NH_3 oxidation in laminar flow quartz reactors may be initiated by surface reactions [26,64]. Following Glarborg [57], we account for this phenomenon in the modeling by introducing 1 ppm of HONO in the reactant mixture for lean and stoichiometric conditions. In some cases, this addition serves to shorten the predicted induction time, but mostly it has only a small impact under the conditions studied here. This is in agreement with the

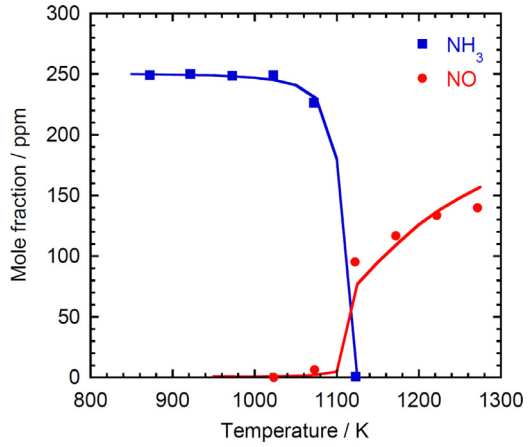

Fig. 1. Comparison of experimental data from Wargadalam et al. [22] and modeling predictions for oxidation of a CO/NH_3 mixture in a premixed, laminar flow quartz reactor. Experimental data are shown as symbols, modeling predictions as lines. Inlet mole fractions: CO = 1250 ppm, NH_3 = 250 ppm, O_2 = 10%; balance N_2. In the calculations, 1 ppm HONO was added in the inlet. The pressure was 1.0 atm and the reaction time was 339/T(K) s (constant mass flow).

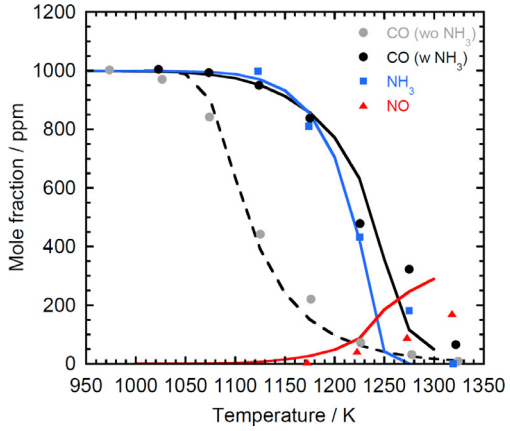

Fig. 2. Comparison of experimental data from Kasaoka et al. [20] and modeling predictions for oxidation of CO and a CO/NH_3 mixture in a premixed, laminar flow quartz reactor. Experimental data are shown as symbols, modeling predictions as lines. Inlet mole fractions: CO = 1000 ppm, NH_3 = 0 or 1000 ppm, O_2 = 5%, H_2O = 10%; balance N_2. In the calculations, 1 ppm HONO was added in the inlet for the CO/NH_3 mixture. The pressure was 1.0 atm and the reaction time in the isothermal zone was assumed to be 18/T(K) s (constant mass flow), as an approximation to their reported temperature profile [65].

findings of Abian et al. [48], who concluded that surface effects were limited under most conditions.

Figure 1 compares the flow reactor results by Wargadalam et al. [22] for NH_3 and NO concentrations obtained during oxidation of ammonia in the presence of CO. These experiments were carried out to evaluate the formation of NO and N_2O in oxidation of biomass volatiles. For this reason, they were conducted with a comparatively high CO/NH_3 ratio and a large excess of O_2. Oxidation of ammonia is initiated above 1100 K. A significant fraction of the NH_3 is oxidized to NO at higher temperatures; more than 50% above 1200 K. The enhanced yield of radicals in the presence of CO promotes NO formation compared to N_2. The kinetic model captures quite accurately the observed profiles for NH_3 and NO.

Whereas Wargadalam et al. conducted their experiments under dry conditions, Kasaoka et al. [20] reported results for CO/NH_3 oxidation in the presence of 10% H_2O. Figure 2 compares their results for oxidation of CO without and with the addition of NH_3. Their results were obtained in a flow reactor with the temperature varying about 100 K over the reaction zone [65]. In the calculations, we have approximated the condition as that of an isothermal reactor with a residence time corresponding roughly to that at their reported peak temperature.

The results of Fig. 2 illustrates an important aspect of the CO/NH_3 oxidation chemistry: that the presence of NH_3 inhibits CO oxidation, here shifting the temperature of reaction more than 100 K to higher values. As discussed in more detail below, the inhibition of CO oxidation by NH_3 is caused by competition for OH radicals between CO and NH_3. A similar behavior has been reported for CH_4/NH_3 oxidation [66]. The model describes the observed trends well. The overprediction of NO at high temperature may partly be attributed to the temperature profile approximation used in the modeling.

Wargadalam et al. [22] and Kasaoka et al. [20] conducted their experiments with oxygen concentrations of 5–10%, corresponding to very lean conditions. To expand the investigated range of conditions, experiments were conducted in the present work at low O_2 levels, ranging from 400 to 6000 ppm, varying also stoichiometry and inlet CO concentration. Figure 3 shows results where the inlet NH_3 was maintained at 1000 ppm, while CO was varied between 200 and 8000 ppm. The O_2 concentration was increased with CO to maintain an overall excess air ratio of $\lambda \sim 1$.

Increasing the concentration of CO and O_2 results in a shift towards lower temperature of the onset of NH_3 conversion and formation of NO. The effect of increasing the inlet CO concentration is more pronounced from 200 to 1000 ppm CO than from 1000 to 8000 ppm CO. The modeling predictions are in satisfactory agreement with the experimental results, but the comparisons should be interpreted cautiously. At the lower CO inlet levels (200 and 1000 ppm) the addition of 1 ppm of HONO in the reactant mixture lowers the predicted onset temperature by about 100 K, indicating that these results may be sensitive to surface initiation. Figure SM3 in the Supplementary Material compares predictions with and without HONO addition. At the highest CO concentration, addition of HONO in the reactant mixture has little impact on predictions. However, this set has a significant adiabatic temperature increase. The deviation observed for NO and N_2 at temperatures above 1150 K may be affected by the uncertainty in the temperature as well as by the finite rate mixing of reactants at the inlet to the reaction zone.

Figure 4 shows concentrations of CO, NH_3, NO, and N_2 as a function of temperature in oxidation of CO/NH_3 mixtures under close to stoichiometric ($\lambda = 1.07$) and lean ($\lambda = 5.6$) conditions. The excess air ratio was controlled by changing the inlet O_2, keeping inlet CO and NH_3 of approximately 1000 ppm. The conversion of ammonia increases with temperature and inlet O_2 level. Compared to results obtained in the absence of CO (see Fig. SM1 in the Supplementary Material), addition of 1000 ppm CO shifts the conversion of ammonia by 25–75 K to lower temperature. The CO oxidation serves to replenish the radical pool and thereby promote consumption of NH_3.

Conversion of CO to CO_2 occurs at roughly the same temperature as for ammonia. Nitric oxide is formed in significant quantities at both near-stoichiometric and lean conditions. The modeling predictions for CO, NH_3, and NO are in good agreement with the experiment. The main deviation occurs for NO, which is overpredicted under lean conditions at the highest temperatures; we attribute this discrepancy mainly to the mixing limitations in the experiments.

Figure 5 shows results for CO/NH_3 oxidation under reducing conditions ($\lambda = 0.34$). The results obtained in the present work are compared with data from Abian et al. [48] for NH_3 oxidation in the absence of CO. The NH_3 consumption slowly increases with temperature above 1100 K, but never reaches a fast oxidation regime. The presence of CO apparently has only a small impact on NH_3 oxidation; the NH_3 profiles are similar for the two conditions. Below

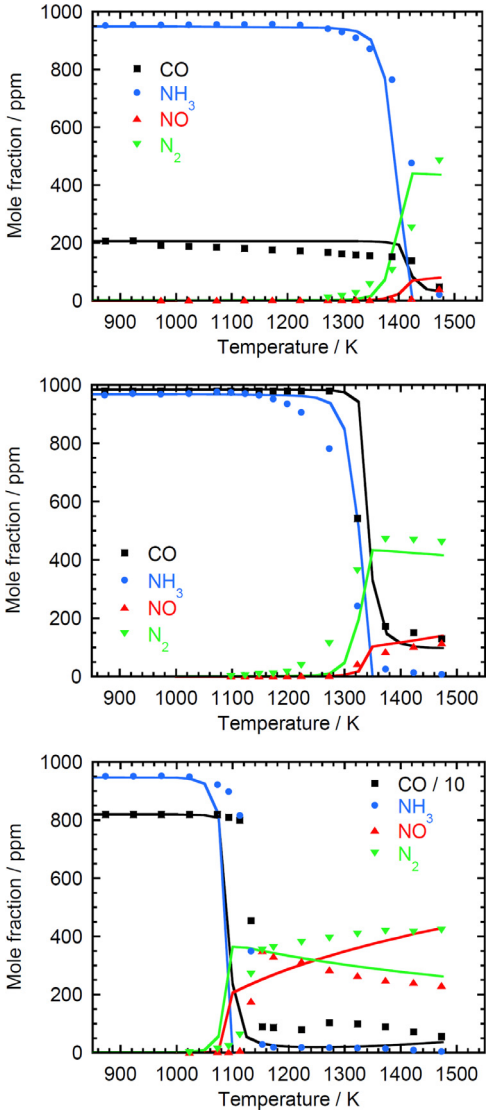

Fig. 3. Comparison of experimental data (pw) and modeling predictions for oxidation of a CO/NH_3 mixture in a quartz flow reactor: effect of CO inlet concentration (constant overall stoichiometry). Experimental data are shown as symbols, modeling predictions as lines. Inlet mole fractions, *top*: CO = 206 ppm, NH_3 = 951 ppm, O_2 = 910 ppm; *middle*: CO = 985 ppm, NH_3 = 970 ppm, O_2 = 1360 ppm; *bottom*: CO = 8190 ppm, NH_3 = 950 ppm, O_2 = 5128 ppm. In the calculations, 1 ppm HONO was added in the inlet. In all experiments, Ar was used as carrier gas and the pressure was 1.0 atm. The reaction time was 180/T(K) s (constant mass flow).

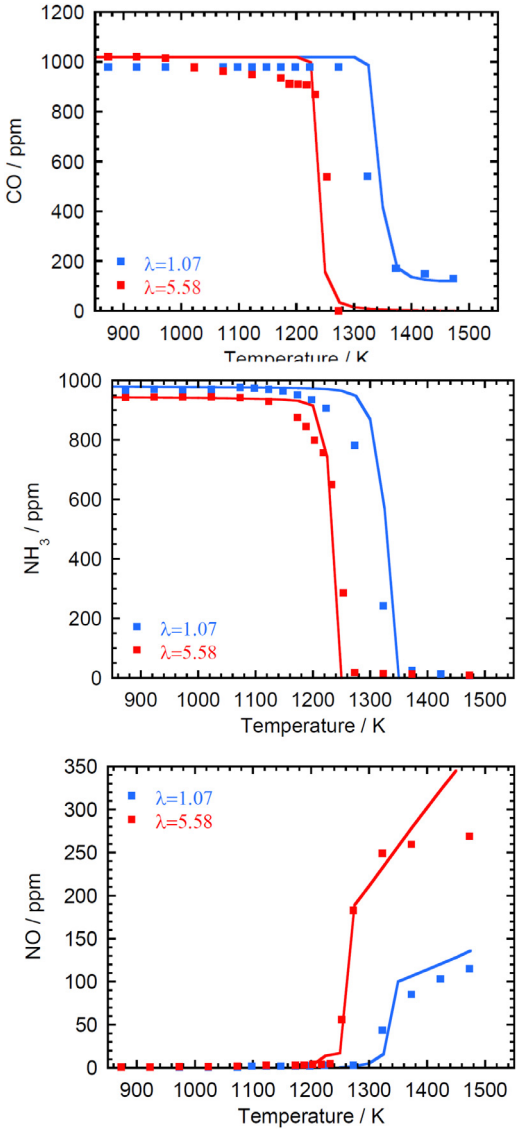

Fig. 4. Comparison of experimental data (pw) and modeling predictions for oxidation of a NH_3/CO mixture in a quartz flow reactor: effect of stoichiometry. Experimental data are shown as symbols, modeling predictions as lines. Inlet mole fractions for λ = 1.07: CO = 1024 ppm, NH_3 = 979 ppm, O_2 = 1331 ppm; λ = 5.58: CO = 1020 ppm, NH_3 = 943 ppm, O_2 = 6793 ppm. In the calculations, 1 ppm HONO was added in the inlet. In all experiments, Ar was used as carrier gas and the pressure was 1.0 atm. The reaction time was 180/T(K) s (constant mass flow).

1300 K, CO is consumed, while above this temperature, consumption of CO and NH_3 is comparable. Formation of NO is negligible under reducing conditions.

The model does not capture the measured concentration profiles under reducing conditions. Contrary to observation, very little reaction is predicted both in the absence and presence of CO, even at the highest temperatures. Potential reasons for the short-coming of the model for reducing conditions are discussed below.

The model reproduces well the main trends observed experimentally under stoichiometric and lean conditions and is therefore used to further analyze the present results. Figure 6 shows a reaction pathway diagram for NH_3 oxidation under the conditions of Figs. 1–5. Ammonia is converted to NH_2 by reaction mainly with OH. The NH_3 + OH reaction competes directly with CO + OH for the hydroxyl radical. The fate of NH_2 depends strongly on the excess air ratio, the relative levels of NH_3 and CO, and the amount of NO formed.

Under stoichiometric and lean conditions, NH_2 is mostly oxidized to NO, through either NH or HNO. Once NO is formed in sufficient amounts, the NH_2 + NO reaction becomes the major consumption path for NH_2, with NH_2 + O_2 being too slow to play a role except at very high temperature. At very lean conditions (Fig. 1), HO_2 is formed in significant concentrations by the reaction of HNO with O_2, and the fast reaction $NH_2 + HO_2 \rightarrow NH_3 + O_2$ becomes an important chain-terminating step. A fraction of the NH_2 + HO_2 reaction yields H_2NO, which is largely recycled back to NH_2 by reaction with atomic oxygen.

Due to the poor agreement between experiments and modeling predictions, the reaction path analysis for reducing conditions (Fig. 5) must be interpreted with caution. However, the analysis indicates that amine-amine reactions feeding into the N_2-amine pool become more important, in particular $NH_2 + NH \rightarrow$ tHNNH + H at high temperature.

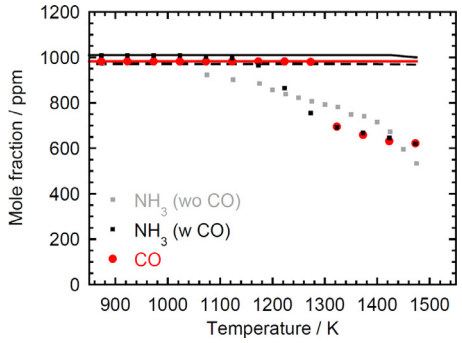

Fig. 5. Comparison of experimental data (pw) and modeling predictions for oxidation of NH_3 [48] and CO/NH_3 mixture (pw) in a quartz flow reactor under reducing conditions. Experimental data are shown as symbols, modeling predictions as lines. Data for NH_3 oxidation are shown as open symbols and a dashed line, while those in presence of CO are shown as solid symbols and solid lines. Inlet mole fractions: NH_3 = 971 ppm, O_2 = 298 ppm ($\lambda = 0.4$); balance N_2, or CO = 982 ppm, NH_3 = 1008 ppm, O_2 = 422 ppm ($\lambda = 0.34$); balance Ar. The pressure was 1.0 atm and the reaction time was 195/T(K) s (without CO) or 180/T(K) s (with CO).

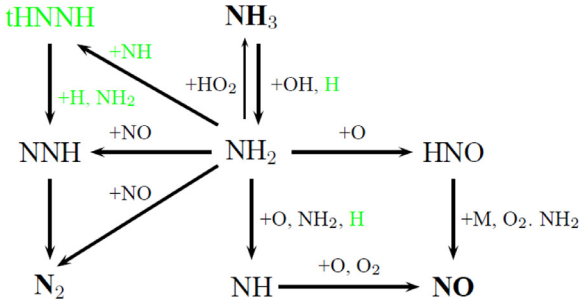

Fig. 6. Reaction path diagram for oxidation of NH_3 in the presence of CO. The species and pathways marked in green are important only under reducing conditions. (For interpretation of the references to color in this figure legend, the reader is referred to the web version of this article.)

Figure 7 shows the results of a sensitivity analysis for NH_3 under reducing, stoichiometric, and lean conditions, respectively. Progress of reaction is largely determined by competition between chain branching and chain terminating sequences. The competition for radicals between CO and NH_3 is important; CO + OH → CO_2 + H promotes oxidation, while NH_3 + OH → NH_2 + H_2O inhibits reaction, because H is a more reactive radical than NH_2. Another important competition is between H + O_2 → O + OH (branching) and H + O_2 (+M) → HO_2 (+M) (in effect terminating). In a similar way, NH_3 + H slows down reaction by competing for atomic H with H + O_2, while NH_3 + O → NH_2 + OH is branching and promotes oxidation. Finally, even in the absence of NO in the inlet, the competition between NH_2 + NO → NNH + NO (branching) and NH_2 + NO → N_2 + H_2O (terminating) shows up as important.

The reaction path and sensitivity analyses do not provide clear indications of the reason for the poor agreement under reducing conditions between experiment and prediction. As discussed above, the measured NH_3 profile shows a comparatively low reaction rate, increasing slowly with temperature; there is no apparent transition to a regime with fast reaction governed by chain-branching. An important feature is that only NH_3 is consumed below 1300 K; above this temperature CO and NH_3 are oxidized at comparable rates.

To identify possible reasons for the discrepancy, we look closer at the key reactions. If we disregard the presence of the small amount of O_2, the ammonia conversion happens through the sequence NH_3 + H → NH_2 + H_2, NH_2 + H/NH_2 → NH + H_2/NH_3, NH_2 + NH → HNNH + H, HNNH + H/NH_2 → N_2 + H + H_2/NH_3. This sequence is strongly terminating, removing four chain carriers, and if it dominates, very little reaction will occur. Reactions involving formation of O and OH radicals are required to break the terminating cycle and introduce chain branching below 1400 K, where thermal dissociation of NH_3 and HNNH is slow. While the rate constant for H + O_2 is comparable at 1300 K with that of NH_3 + H, the latter step dominates because ammonia is present in a larger concentration. Both NH_3 + O_2, NH_2 + O_2, and presumably also HNNH + O_2 are slow reactions that cannot compete in this temperature range. The NH + O_2 reaction is faster, but cannot by itself provide the branching needed.

Apparently, changes of rate constants in the mechanism within their uncertainty limits cannot eliminate the discrepancy between experiment and prediction under reducing conditions (Fig. 5). Even an assumption of prompt dissociation of HNNH, so the NH_2 + NH reaction essentially yields N_2 + 3H, does not change predictions compared to the basis model. Since N_2-amines are formed largely

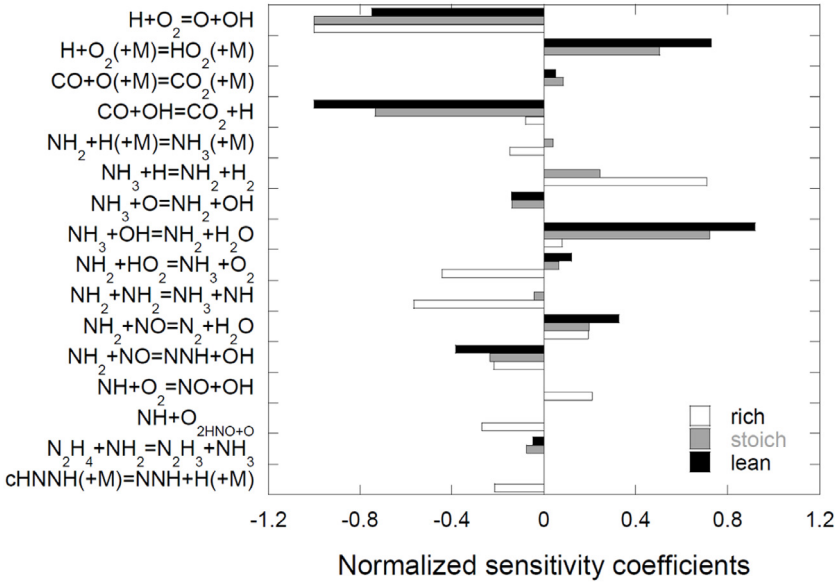

Fig. 7. Sensitivity of NH_3 to key reactions for oxidation of CO/NH_3 mixtures. Conditions correspond to the fuel-rich set in Fig. 5 ($\lambda = 0.34$, 1350 K; prolonged residence time); the stoichiometric set in Fig. 3 (CO = 8190 ppm, 1000 K); and the lean set in Fig. 1 (1100 K).

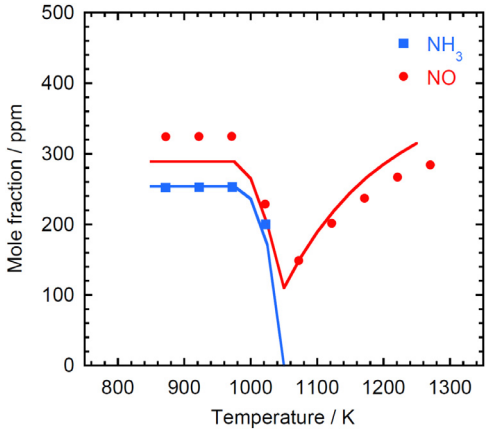

Fig. 8. Comparison of experimental data from Wargadalam et al. [22] and modeling predictions for oxidation of a CO/NH_3/NO mixture in a quartz flow reactor. Experimental data are shown as symbols, modeling predictions as lines. Inlet mole fractions: CO = 1290 ppm, NH_3 = 254 ppm, NO = 289 ppm, O_2 = 10%; balance N_2. The pressure was 1.0 atm and the residence time given as 339/T(K) s (constant mass flow).

by NH_2 + NH, and thereby requires formation of NH, they are only important at high temperatures, and changes in this subset apparently cannot bring the modeling predictions in accord with observations.

Addition of 1 ppm N_2H_4 or other possible promoters in the inlet to simulate surface initiation facilitates reaction only at high temperature where the chain-terminating steps listed above no longer dominate. This indicates that the discrepancy under reducing conditions is not an initiation problem. More work is required to resolve this issue.

4.2. Effect of CO on NH_3 oxidation in the presence of NO

Nitric oxide will be present in the burnout region in an ammonia-fueled engine, and for this reason the chemistry will resemble that of selective non-catalytic reduction (SNCR) of NO. Characteristic of this process is that NO removal is possible only in a narrow temperature range centered at 1250 K and only in the presence of oxygen [25,26]. At temperatures above 1400 K, reactions of NH_2 with the radical pool become dominant and NH_3 is oxidized to NO rather than to N_2.

Similar to the flow reactor studies of CO/NH_3 oxidation, most results reported for the effect of CO on SNCR with NH_3 were obtained at high O_2 concentrations, typically 2–10%. Figure 8 compares the flow reactor results by Wargadalam et al. [22] for the NH_3-NO-O_2 reaction in the presence of CO under conditions similar to those of Fig. 1, i.e., dry with 10% O_2. Due to the promoting effect of CO, the characteristic temperature window for NO reduction is here located at 1000–1200 K. The onset of NO reduction coincides with a rapid consumption of NH_3. The kinetic modeling reproduces well both the NH_3 conversion and the NO reduction.

Figure 9 shows results from Alzueta et al. [37] for ammonia conversion under moist conditions in the presence of both NO and CO. These experiments, designed to study hybrid reburn-SNCR strategies, were conducted with CO levels ranging from 0 to 2.1%. Since the O_2 concentration was kept constant in the experiments, the increase in CO resulted in an excess air ratio λ that decreased from 180 to 3. Varying the concentration of CO from 0 ppm to 2.1% produces a shift of more than 300 K in the low-temperature boundary for the process. The NO reduction potential, 65–70%, is roughly independent of the CO concentration, but the temperature window for NO reduction gets more narrow as the CO level increases. The minimum in NO concentration coincides roughly with the steepest gradient in NH_3. Again, there is a good agreement between experimental results and model calculations, particularly in the presence of CO. The model predicts well the onset of NH_3 consumption and the NO reduction, as well as the shape of the concentration profiles. The differences observed in the upper part of the temperature window for each set may partly be attributed to finite rate mixing effects in the experiments.

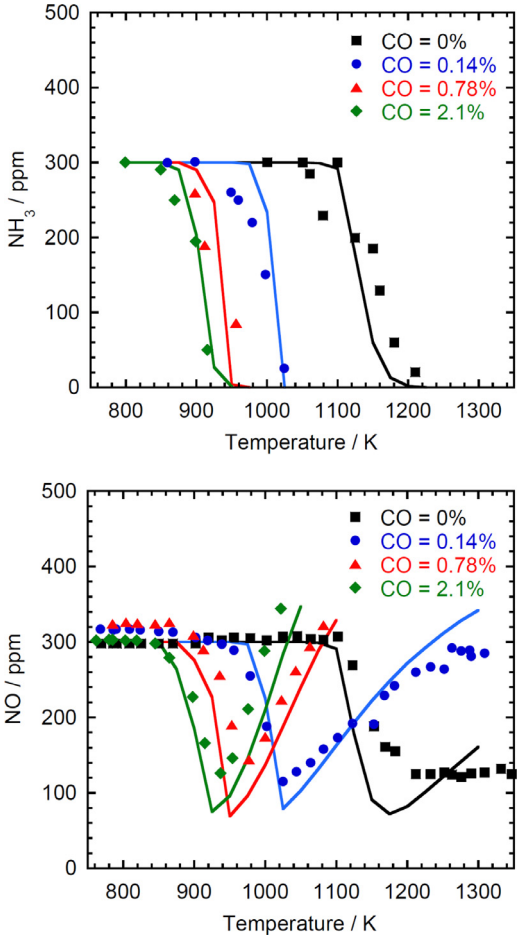

Fig. 9. Comparison of experimental data from Alzueta et al. [37] and modeling predictions for the effect of CO inlet concentration on the reduction of NO by NH_3 in a quartz flow reactor. Symbols denote experimental data, while solid lines denote modeling predictions. Inlet concentrations: 300 ppm NH_3, 300 ppm NO, 4.0% O_2, 4.5% H_2O; balance N_2. Pressure is 1.1 atm and the residence time given as 180/T(K) s (constant mass flow).

Suhlmann and Rotzoll [35] investigated the effect of the CO concentration on the SNCR process at a fixed temperature. Figure 10 shows results for a mixture of 1500 ppm NH_3, 1000 ppm NO, and 3% O_2, with varying CO and an oven temperature setting of 1048 K. At an inlet CO level of 0.4% there is a sharp onset of reaction, with the NH_3 fully converted at 0.45% CO. The behavior is captured well by the model. Predictions are shown both for isothermal and adiabatic conditions, but the difference is not large. Under adiabatic conditions, the heat release from the slow conversion of CO to CO_2 serves to raise the temperature sufficiently to facilitate reaction at a slightly lower level of CO.

To extend the experimental database to a wider range of mixture compositions, novel experiments were conducted for NH_3 oxidation in the presence of both CO and NO. These experiments were conducted with inlet O_2 concentrations of 400–7000 ppm, well below the levels in most studies of SNCR in the literature. Figure 11 shows the effect of increasing the inlet CO and O_2 concentrations at constant excess air ratio (close to stoichiometric). The maximum NO reduction achieved decreases with the concentration of CO, and

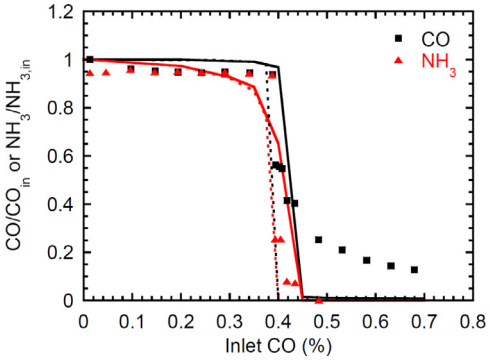

Fig. 10. Comparison of experimental data from Suhlmann and Rotzoll [35] and modeling predictions for conversion of CO and NH_3 in a $CO/NH_3/NO/O_2/N_2$ mixture as a function of the inlet CO concentration under flow reactor conditions. Experimental data are shown as symbols. Isothermal modeling predictions are shown as solid lines, while adiabatic calculations are shown as dashed lines. Inlet mole fractions: NH_3 = 1500 ppm, NO = 1000 ppm, O_2 = 3%; balance N_2. P = 1.0 atm. The reactor temperature was 1048 K and the reaction time was 0.53 s.

at 8000 ppm CO the amount of NO removed is negligble. The concentration of chain carriers increases with the reactant concentrations; higher radical levels promote oxidation of NH_3 to NO compared to oxidation to N_2.

The model predictions at the highest inlet CO level become sensitive to recombination reactions of CO, both CO + O (+M) ⇄ CO_2 (+M) and CO + H (+M) ⇄ HCO (+M). The HCO formed is rapidly recycled to CO by reaction with the radical pool.

Figure 12 shows concentrations of CO, NH_3, and NO as a function of temperature and stoichiometry. The conversion of ammonia is promoted by higher temperature and higher oxygen availability. Under lean and stoichiometric conditions, the presence of 1000 ppm NO results in a shift of about 100 K for the onset of ammonia conversion to lower temperatures, compared to the results obtained under similar conditions without NO in the inlet (Fig. 4). The addition of 1000 ppm CO has a similar impact (see Fig. SM2 in the Supplementary Material).

Calculations indicate that conversion of ammonia is mainly driven by the concentration level of the radical pool, which is increased in the presence of CO and even more with both CO and NO together. In fact, the sharp conversion of ammonia occurring in a narrow temperature interval only occurs under conditions with both CO and NO present (e.g., Figs. 12 and SM2).

Even under reducing conditions, modeling predictions agree well with the measurements. Unlike the behavior under stoichiometric and lean conditions, the presence of NO here leads to inhibition, shifting the onset temperature for NH_3 conversion to higher values compared to the results in Fig. 4. The inhibition caused by NO for $\lambda = 0.35$ may at least partly be attributed to the chain terminating sequence H + NO (+M) ⇄ HNO (+M), HNO + H ⇄ NO + H_2.

Figure 13 shows a reaction path diagram for NH_3 oxidation in the presence of NO. Consumption of NH_2 occurs almost entirely by reaction with NO, except at high temperatures where NH_2 + radical reactions begin to compete. Under lean conditions, nitric oxide is formed through NH_2 + O → HNO + O, followed by reaction of HNO with radicals or O_2 to form NO. Under reducing conditions, nitrous oxide is formed through the sequence NH_2 + H → NH +H_2, NH + NO → N_2O + H.

Figure 14 shows the results of a sensitivity analysis for the $CO/NH_3/NO/O_2$ system. The key reactions are largely the same over the range of stoichiometry, and they are similar also to those of CO/NH_3 oxidation (Fig. 7), but their relative importance varies. The production of chain carriers is controlled by the fast NH_2 + NO reaction, and predictions are very sensitive to the branching fraction for the reaction, defined as the fractional yield of NNH. There is also a high sensitivity to the competition between H + O_2 ⇄ O + OH and H + O_2 (+M) ⇄ HO_2 (+M), and between CO and NH_3 for OH radicals.

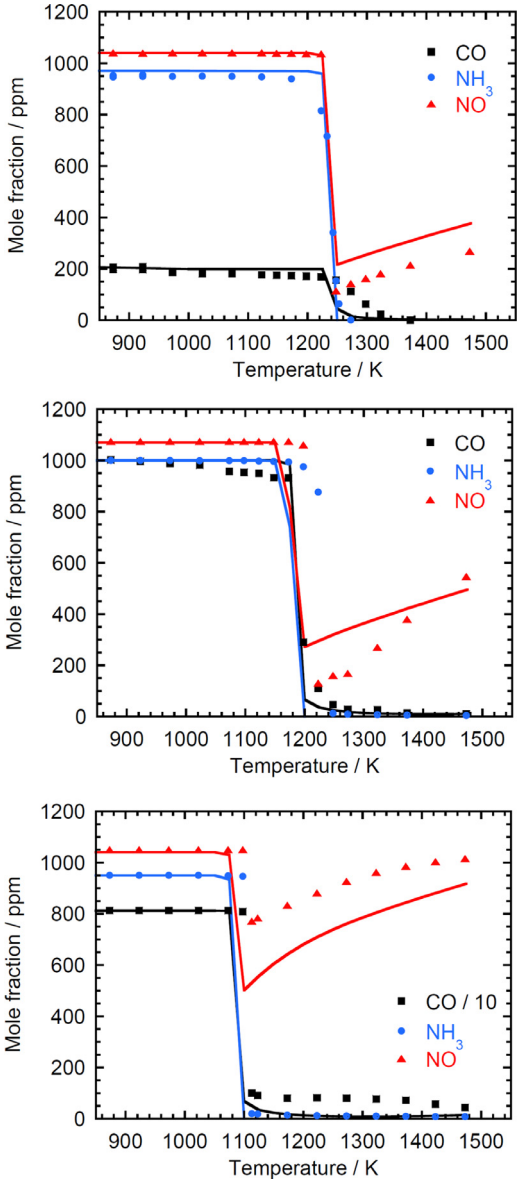

Fig. 11. Comparison of experimental data (pw) and modeling predictions for oxidation of a $CO/NH_3/NO$ mixture in a quartz flow reactor: effect of CO inlet concentration (constant overall stoichiometry). Experimental data are shown as symbols, modeling predictions as lines. Inlet mole fractions, *top*: CO = 199 ppm, NH_3 = 970 ppm, NO = 1040 ppm, O_2 = 890 ppm; *middle*: CO = 1002 ppm, NH_3 = 1000 ppm, NO = 1074 ppm, O_2 = 1375 ppm; *bottom*: CO = 8120 ppm, NH_3 = 950 ppm, NO = 1050 ppm, O_2 = 5098 ppm. In all experiments, Ar was used as carrier gas and the pressure was 1.0 atm. The reaction time was 180/T(K) s (constant mass flow).

4.3. Effect of CO on NH_3 flame speed

Unlike the behavior in flow reactors, the chemistry in laminar premixed flames is independent of initiation and results from flames are important for model validation. The flame speed of CO/NH_3 mixtures has been measured by Han et al. [8] and Wang et al. [10] over a range of stoichiometry and pressure. Figure 15 compares their data as a function of fuel-air equivalence ratio (ϕ), fuel composition, and pressure (1–5 bar) with modeling predic-

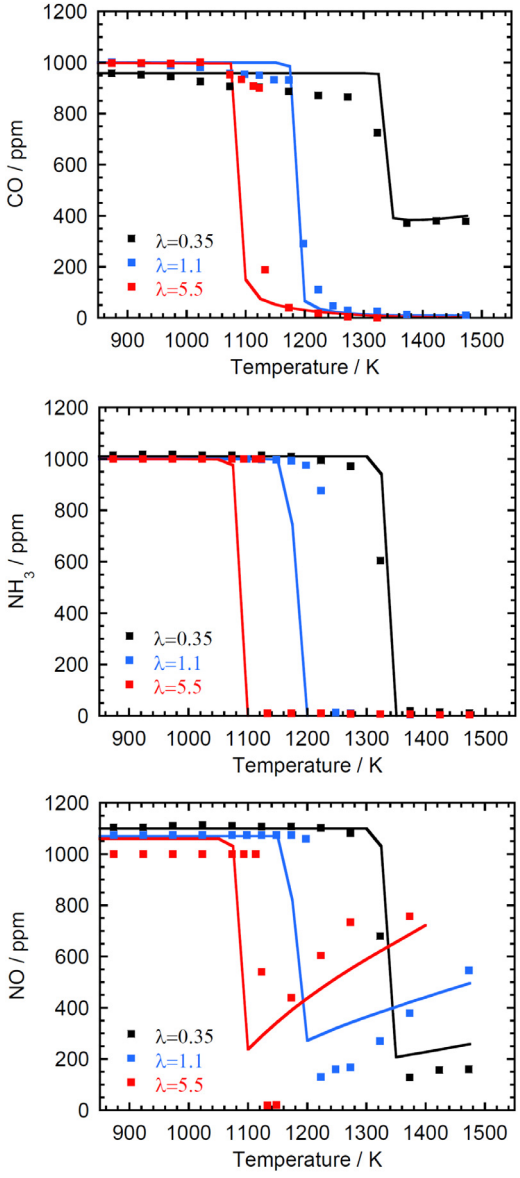

Fig. 12. Comparison of experimental data (pw) and modeling predictions for oxidation of a NH_3/CO mixture in a quartz flow reactor. Experimental data are shown as symbols, modeling predictions as lines. Inlet mole fractions for $\lambda = 0.35$: CO = 958 ppm, NH_3 = 1014 ppm, NO = 1104 ppm, O_2 = 435 ppm; $\lambda = 1.1$: CO = 1002 ppm, NH_3 = 1000 ppm, NO = 1074 ppm, O_2 = 1375 ppm; $\lambda = 5.58$: CO = 998 ppm, NH_3 = 999 ppm, NO = 1056 ppm, O_2 = 6905 ppm. In all experiments, Ar was used as carrier gas and the pressure was 1.0 atm. The reaction time was 180/T(K) s (constant mass flow).

tions. The flame speed of neat NH_3 in air is below 7 cm s^{-1}. Increasing the CO share of the fuel mixture accelerates the flame propagation significantly. Where the CO fraction is smaller than the NH_3 fraction, the flame speed profile peaks at around $\phi = 1.05$, but for larger CO ratios, the peak location shifts to more reducing conditions, with a value of $\phi = 1.45$ for 80% CO. The shift in peak to more fuel-rich mixtures at high CO fractions can be attributed mostly to the reduction in the heat capacity of the reactant mixture, allowing an increase in flame temperature. An increase in pressure serves to decelerates the flame propagation.

It is a known short-coming of the mechanism of Glarborg et al. [26] that it overpredicts laminar flame speeds for neat NH_3 as fuel (see the discussion in Valera-Medina et al. [3]). The present mechanism provides a better prediction of the NH_3 flame speed, even though it is still higher than experiment. When CO is added to the

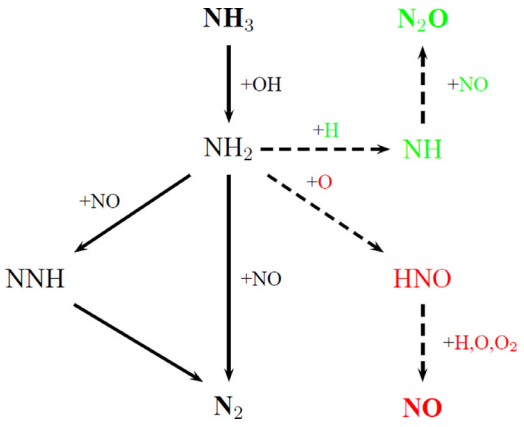

Fig. 13. Reaction path diagram for the SNCR process. Dashed lines denote pathways only important at high temperatures; species marked in green or red important only under reducing or oxidizing conditions, respectively. (For interpretation of the references to color in this figure legend, the reader is referred to the web version of this article.)

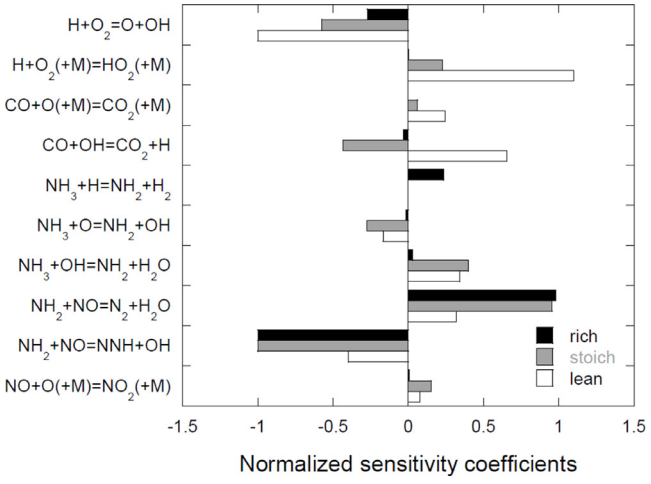

Fig. 14. Sensitivity of NH_3 to key reactions in SNCR. Conditions correspond to the rich set in Fig. 12 ($\lambda = 0.35$, 1350 K); the stoichiometric set in Fig. 11 (CO = 8120 ppm, 1025 K); and the lean set in Fig. 9 (CO = 2.1%, 900 K).

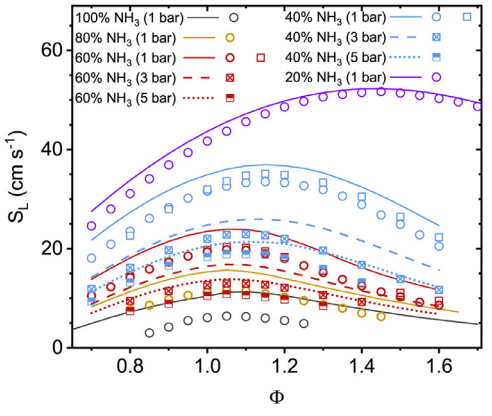

Fig. 15. Laminar burning velocity of CO/NH_3/air mixtures as a function of dilution and fuel-air equivalence ratio. Symbols denote experimental data from Han et al. [8] (circles) and Wang et al. [10] (squares). Lines show the prediction of the present model.

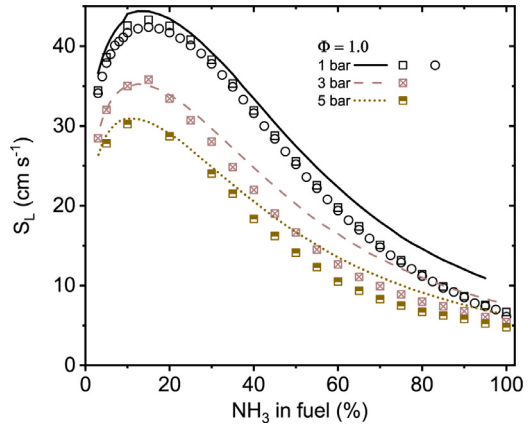

Fig. 16. Laminar burning velocity of stoichiometric CO/NH_3/air mixtures as a function of NH_3/CO ratio in the fuel. Symbols denote experimental data from Han et al. [8] (circles) and Wang et al. [10] (squares). Lines show the prediction of the present model.

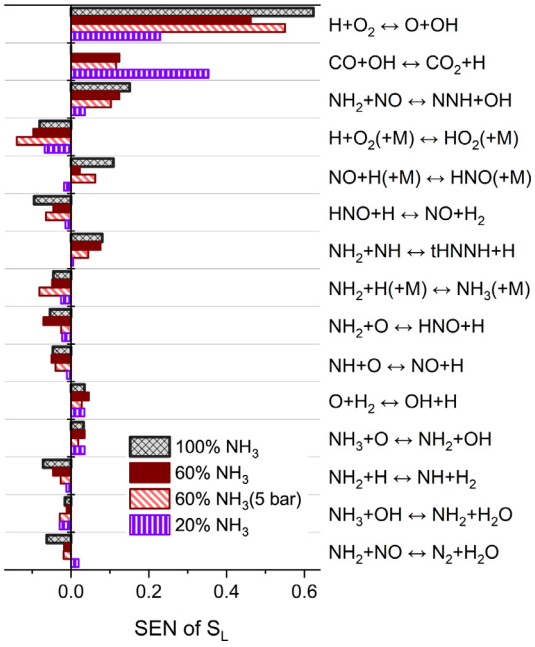

Fig. 17. Sensitivity of laminar burning velocity of stoichiometric CO/NH_3/air mixtures to reaction rate constants.

NH_3 fuel mixture, the modeling predictions are in good agreement with the measured results. Contrary to the flow reactor results discussed above, there is no deterioration in the agreement between calculations and experiment under reducing conditions.

Figure 16 shows the effect of the ammonia fuel fraction on the flame speed for a stoichiometric mixture. For CO levels smaller than 10–15% of the fuel mixture, the flame speed increases with CO/NH_3 ratio. In contrast, increase of the CO fuel fraction above 15% reduces the flame speed dramatically. The model is able to reproduce the flame speed for mixtures with a high CO/NH_3 ratio fairly accurately, but the agreement deteriorates at higher NH_3 fractions.

Figure 17 shows the sensitivity coefficients for the predicted flame speed for different mixtures of CO/NH_3/air. Similar to the oxidation rate in the flow reactor, the predicted flame speed is very sensitive to the rate coefficients for reactions leading to chain branching, in particular CO + OH ⇄ CO_2 + H, H + O_2 ⇄ O + OH, and NH_2+NO ⇄ NNH+OH. The chain terminating reactions NH_2+O ⇄ HNO+H and NO+H(+M) ⇄ HNO(+M) show the largest sensitivity to a pressure raise from 1 to 5 bar.

5. Conclusions

A detailed chemical kinetic model for ammonia oxidation in the presence of carbon monoxide has been revised, based on recent theoretical and experimental results, and tested against a wide range of experimental data from flow reactors and flames. Literature data for very lean conditions are supplemented in the present work with novel flow reactor data on CO/NH_3 and CO/NH_3/NO oxidation at comparatively low O_2 levels, varying temperature (850–1475 K), reactant level (200–8000 ppm CO), and excess air ratio (0.34-5.6). The agreement between prediction and experiment is good, except at reducing conditions in the absence of NO where reaction is underpredicted. The model also provides a good prediction of CO/NH_3 flame speeds as a function of stoichiometry, fuel mixture, and pressure, even though the accuracy deteriorates for very low CO/NH_3 fuel ratios where the flame speed is overpredicted. The work serves to validate the amine subset of the reaction mechanism under the investigated conditions and offers a kinetic model that can be used reliably for post-flame oxidation modeling in engines and gas turbines fueled by ammonia with a hydrocarbon or alcohol as co-fuel.

Declaration of Competing Interest

The authors declare that they have no known competing financial interests or personal relationships that could have appeared to influence the work reported in this paper.

Acknowledgments

This publication is part of the Project RTI2018-098856-B-I00 financed by MCIN/AEI/10.13039/501100011033/FEDER “Una manera de hacer Europa”. MUA and IS express their gratitude to Aragon Government (Ref. T22_20R), cofounded by FEDER 2014–2020 “Construyendo Europa desde Aragon”. HH and PG would like to acknowledge funding from Innovation Fund Denmark for the AEngine Grand Solutions project.

Supplementary material

Supplementary material associated with this article can be found, in the online version, at doi:10.1016/j.combustflame.2022.112438

References

[1] H. Kobayashi, A. Hayakawa, K.K.A. Somarathne, E.C. Okafor, Science and technology of ammonia combustion, Proc. Combust. Inst. 37 (2019) 109–133.
[2] A. Valera-Medina, H. Xiao, M. Owen-Jones, W.I.F. David, P.J. Bowen, Ammonia for power, Prog. Energy Combust. Sci. 69 (2018) 63–102.
[3] A. Valera-Medina, F. Amer-Hatem, A. Azad, I. Dedoussi, M.D. Joannon, R. Fernandes, P. Glarborg, H. Hashemi, X. He, S. Mashurk, J. McGowan, C. Mounaim-Rouselle, A. Ortiz-Prado, J.A. Ortiz-Valera, I. Rossetti, B. Shu, M. Yehia, H. Xiao, M. Costa, A review on ammonia as a potential fuel: from synthesis to economics, Energy Fuels 35 (2021) 6964–7029.
[4] J. Bian, J. Vandooren, P.J. Van Tiggelen, Experimental study of the formation of nitrous and nitric oxides in H_2 - O_2 - Ar flames seeded with NO and/or NH_3, Symp. (Int.) Combust. 23 (1991) 379–386.
[5] J. Vandooren, Comparison of the experimental structure of an ammonia seeded rich hydrogen-oxygen-argon flame with the calculated ones along several reaction mechanisms, Combust. Sci. Technol. 84 (1992) 335–344.
[6] C. Duynslaegher, H. Jeanmart, J. Vandooren, Flame structure studies of premixed ammonia/hydrogen/oxygen/argon flames: experimental and numerical investigation, Proc. Combust. Inst. 32 (2009) 1277–1284.
[7] P. Kumar, T.R. Meyer, Experimental and modeling study of chemical-kinetics mechanisms for H_2–NH_3–air mixtures in laminar premixed jet flames, Fuel 108 (2013) 166–176.
[8] X. Han, Z. Wang, M. Costa, Z. Sun, Y. He, K. Cen, Experimental and kinetic modeling study of laminar burning velocities of NH_3/air, NH_3/H_2/air, NH_3/CO/air and NH_3/CH_4/air premixed flames, Combust. Flame 206 (2019) 214–226.
[9] C. Lhuillier, P. Brequigny, N. Lamoureux, F. Contino, C. Mounaïm-Rousselle, Experimental investigation on laminar burning velocities of ammonia/hydrogen/air mixtures at elevated temperatures, Fuel 263 (2020) 116653.

[10] S. Wang, Z. Wang, A.M. Elbaz, X. Han, Y. He, M. Costa, A.A. Konnov, W.L. Roberts, Experimental study and kinetic analysis of the laminar burning velocity of NH_3/syngas/air, NH_3/CO/air and NH_3/H_2/air premixed flames at elevated pressures, Combust. Flame 221 (2020) 270–287.
[11] K.P. Shrestha, C. Lhuillier, A.A. Barbosa, P. Brequigny, F. Contino, C. Mounaïm-Rousselle, L. Seidel, F. Mauss, An experimental and modeling study of ammonia with enriched oxygen content and ammonia/hydrogen laminar flame speed at elevated pressure and temperature, Proc. Combust. Inst. 38 (2021) 2163–2174.
[12] B. Mei, J. Zhang, X. Shi, Z. Xi, Y. Li, Enhancement of ammonia combustion with partial fuel cracking strategy: laminar flame propagation and kinetic modeling investigation of $NH_3/H_2/N_2$/air mixtures up to 10 atm, Combust. Flame 231 (2021) 111472.
[13] N. Wang, S. Huang, Z. Zhang, T. Li, P. Yi, D. Wu, G. Chen, Laminar burning characteristics of ammonia/hydrogen/air mixtures with laser ignition, Int. J. Hydrogen Energy 46 (2021) 31879–31893.
[14] G.J. Gotama, A. Hayakawa, E.C. Okafor, R. Kanoshima, M. Hayashi, T. Kudo, H. Kobayashi, Measurement of the laminar burning velocity and kinetics study of the importance of the hydrogen recovery mechanism of ammonia/hydrogen/air premixed flames, Combust. Flame 236 (2022) 111753.
[15] K.N. Osipova, O.P. Korobeinichev, A.G. Shmakov, Chemical structure and laminar burning velocity of atmospheric pressure premixed ammonia/hydrogen flames, Int. J. Hydrogen Energy 246 (2022) 112419.
[16] X. He, B. Shu, D. Nascimento, K. Moshammer, M. Costa, R.X. Fernandes, Auto-ignition kinetics of ammonia and ammonia/hydrogen mixtures at intermediate temperatures and high pressures, Combust. Flame 206 (2019) 189–200.
[17] M. Pochet, V. Dias, B. Moreau, F. Foucher, H. Jeanmart, F. Contino, Experimental and numerical study, under LTC conditions, of ammonia ignition delay with and without hydrogen addition, Proc. Combust. Inst. 37 (2019) 621–629.
[18] L. Dai, S. Gersen, P. Glarborg, H. Levinsky, A. Mokhov, Experimental and numerical analysis of the autoignition behavior of NH_3 and NH_3/H_2 mixtures at high pressure, Combust. Flame 215 (2020) 134–144.
[19] J. Chen, X. Jiang, X. Qin, Z. Huang, Effect of hydrogen blending on the high temperature auto-ignition of ammonia at elevated pressure, Fuel 287 (2021) 119563.
[20] S. Kasaoka, E. Sasaoka, M. Ikoma, Effect of addition of carbon monoxide and hydrogen on non-catalytic reduction of nitrogen monoxide with ammonia, Nippon Kagaku Kaishi (4) (1981) 597–604.
[21] Z.S. Zhao, H. Matsuda, N. Arai, M. Hasatani, Mechanism of NH_3 oxidation in gas system of coexisting CO, Kagaku Kogaku Ronbunshu 18 (1992) 403–412.
[22] V.J. Wargadalam, G. Löffler, F. Winter, H. Hofbauer, Homogeneous formation of NO and N_2O from the oxidation of HCN and NH_3 at 600–1000 °C, Combust. Flame 120 (2000) 465–478.
[23] Y. Wang, J. Zhao, X. Wei, S. Li, Effect of HCl on NO formation during CO/NH_3 combustion in an entrained flow reactor at 1023–1223 K, Energy Fuels 31 (2017) 3281–3287.
[24] K.T. Oganesyan, A.B. Nalbandyan, Determination of the rate constants in the reactions of H and O atoms with the NH_3 molecule, Dokl. Akad. Nauk 160 (1965) 162–165.
[25] J.A. Miller, C.T. Bowman, Mechanism and modeling of nitrogen chemistry in combustion, Prog. Energy Combust. Sci. 15 (1989) 287–338.
[26] P. Glarborg, J.A. Miller, B. Ruscic, S.J. Klippenstein, Modeling nitrogen chemistry in combustion, Prog. Energy Combust. Sci. 67 (2018) 31–68.
[27] M.U. Alzueta, L. Ara, V.D. Mercader, M. Delogu, R. Bilbao, Interaction of NH_3 and NO under combustion conditions. Experimental flow reactor study and kinetic modeling simulation, Combust. Flame 235 (2022) 111691.
[28] S. Kasaoka, E. Sasaoka, M. Nagahiro, Non-catalytic reduction of nitrogen monoxide with ammonia and oxidation of ammonia with oxygen under coexistence of hydrogen, Nippon Kagaku Kaishi 5 (1979) 668–674.
[29] R.K. Lyon, J.E. Hardy, Discovery and development of the thermal DeNO$_x$ process, Ind. Eng. Chem. Res. 25 (1986) 19–24.
[30] W. Duo, K. Dam-Johansen, K. Østergaard, The influence of additives on selective non-catalytic reduction of nitric oxide with ammonia, Proceedings of the ACHEMASIA 89, Beijing, China, October 11–17 (1989).
[31] B.L. Duffy, P.F. Nelson, Isotopic labeling studies of the selective non-catalytic reduction of NO with NH_3, Symp. (Int.) Combust. 26 (1996) 2099–2108.
[32] T. Hasegawa, M. Sato, Study of ammonia removal from coal-gasified fuel, Combust. Flame 114 (1998) 246–258.
[33] Q. Cao, S. Wu, H. Lui, D. Liu, P. Qiu, Experimental and modeling study of the effects of multicomponent gas additives on selective non-catalytic reduction process, Chemosphere 76 (2009) 1199–1205.
[34] S. Wu, Q. Cao, H. Hui Liu, Q. AN, X. Huang, Experimental and modeling study of the effects of gas additives on the thermal DeNO$_x$ process, Chin. J. Chem. Eng. 18 (2010) 143–148.
[35] J. Suhlmann, G. Rotzoll, Experimental characterization of the influence of CO on the high-temperature reduction of NO by NH_3, Fuel 72 (1993) 175–179.
[36] P. Glarborg, P.G. Kristensen, K. Dam-Johansen, J. Miller, The branching fraction of the NH_2 + NO reaction between 1210 and 1370 K, J. Phys. Chem. 101 (1997) 3741–3745.
[37] M.U. Alzueta, H. Røjel, P.G. Kristensen, P. Glarborg, K. Dam-Johansen, Laboratory study of the Co/NH_3/NO/O_2 system: implications for hybrid reburn/SNCR strategies, Energy Fuels 11 (1997) 716–723.
[38] S.W. Bae, S.A. Roh, S.D. Kim, NO removal by reducing agents and additives in the selective non-catalytic reduction (SNCR) process, Chemosphere 65 (2006) 170–175.
[39] L. Gasnot, D.Q. Dao, J.F. Pauwels, Experimental and kinetic study of the effect of additives on the ammonia based SNCR process in low temperature conditions, Energy Fuels 26 (2012) 2837–2849.
[40] W. Fan, T. Zhu, Y. Sun, D. Lv, Effects of gas compositions on NOx reduction by selective non-catalytic reduction with ammonia in a simulated cement precalciner atmosphere, Chemosphere 113 (2014) 182–187.
[41] T. Yao, Y. Duan, Z. Yang, Y. Li, L. Wang, C. Zhu, Q. Zhou, J. Zhang, M. She, M. Liu, Experimental characterization of enhanced SNCRprocess with carbonaceous gas additives, Chemosphere 177 (2017) 149–156.
[42] J. Zhao, X. Wei, T. Li, S. Li, Effect of HCl and CO on nitrogen oxide formation mechanisms within the temperature window of SNCR, Fuel 267 (2020) 117231.
[43] S. Schmitt, S. Schwarz, L. Ruwe, J. Horstmann, F. Sabath, L. Maier, O. Deutschmann, K. Kohse-Höinghaus, Homogeneous conversion of NO_x and NH_3 with CH_4, CO, and C_2H_4 at the diluted conditions of exhaust-gases of lean operated natural gas engines, Int. J. Chem. Kinet. 53 (2021) 213–229.
[44] J. Chen, W. Fan, X. Wu, S. Liu, H. Guo, Z. Liu, X. Wang, Effects of O_2/CO/CO_2 on NH_3 reducing NO at 1073–1773 K in different flow reactors - Part I: the effect of O_2, Fuel 283 (2021) 119335.
[45] J. Chen, W. Fan, X. Wu, S. Liu, H. Guo, Z. Liu, X. Wang, Effects of O_2/CO/CO_2 on NH_3 reducing NO at 1073–1773 K in different flow reactors - Part II: the effects of CO, CO_2 and the complex atmosphere, Fuel 288 (2021) 119837.
[46] M.U. Alzueta, J.M. Hernández, Ethanol oxidation and its interaction with nitric oxide, Energy Fuels 16 (2002) 166–171.
[47] M.U. Alzueta, R. Pernia, M. Abian, A. Millera, R. Bilbao, CH_3SH conversion in a tubular flow reactor. Experiments and kinetic modelling, Combust. Flame 203 (2019) 23–30.
[48] M. Abián, M. Benés, A. de Goñi, B. Muñoz, M.U. Alzueta, Study of the oxidation of ammonia in a flow reactor. Experiments and kinetic modeling simulation, Fuel 300 (2021) 120979.
[49] M.U. Alzueta, P. Glarborg, K. Dam-Johansen, Low temperature interactions between hydrocarbons and nitric oxide: an experimental study, Combust. Flame 109 (1997) 25–36.
[50] J.M. Colom-Díaz, Á. Millera, R. Bilbao, M.U. Alzueta, Conversion of H_2S/O_2/NO mixtures at different pressures. Experiments and kinetic modeling, Fuel 290 (2021) 120060.
[51] P.G. Kristensen, P. Glarborg, K. Dam-Johansen, Nitrogen chemistry during burnout in fuel-staged combustion, Combust. Flame 107 (1996) 211–222.
[52] A. Stagni, C. Cavallotti, S. Arunthanayothin, Y. Song, O. Herbinet, F. Battin-Leclerc, T. Faravelli, An experimental, theoretical and kinetic-modeling study of the gas-phase oxidation of ammonia, Reaction Chem. Eng. 5 (2020) 696–711.
[53] P. Glarborg, H. Hashemi, S. Cheskis, A.W. Jasper, On the rate constant for NH_2 + HO_2 and third-body collision efficiencies for NH_2 + H (+ M) and NH_2 + NH_2 (+ M), J. Phys. Chem. A 125 (2021) 1505–1516.
[54] P. Marshall, G. Rawling, P. Glarborg, New reactions of diazene and related species for modelling combustion of amine fuels, Mol. Phys. 119 (2021) e1979674.
[55] S.J. Klippenstein, P. Glarborg, Theoretical kinetics predictions for NH_2 + HO_2, Combust. Flame 236 (2022) 111787.
[56] P. Glarborg, H. Hashemi, P. Marshall, Challenges in kinetic modeling of ammonia pyrolysis, Fuel Commun. 10 (2022) 100049.
[57] P. Glarborg, The $NH_3/NO_2/O_2$ system: constraining key steps in ammonia ignition and N_2O formation, Combust. Flame (2022), doi:10.1016/j.combustflame.2022.112311.
[58] A. Lucassen, K. Zhang, J. Warkentin, K. Moshammer, P. Glarborg, P. Marshall, K. Kohse-Höinghaus, Fuel-nitrogen conversion in the combustion of small amines using dimethylamine and ethylamine as biomass-related model fuels, Combust. Flame 159 (2012) 2254–2279.
[59] J.D. Mertens, A.Y. Chang, R.K. Hanson, C.T. Bowman, Reaction kinetics of NH in the shock tube pyrolysis of HNCO, Int. J. Chem. Kinet. 21 (1989) 1049–1067.
[60] J.T. Petty, J.A. Harrison, C.B. Moore, Reactions of trans-hydroxycarbonyl radical studied by infrared spectroscopy, J. Phys. Chem. 97 (1993) 11194–11198.
[61] R.V. Olkhov, Q. Li, M.C. Osborne, I.W.M. Smith, Branching ratios for competing channels in the reaction of HOCO radicals with NO, Phys. Chem. Chem. Phys. 3 (2001) 4522–4528.
[62] G. Poggi, J.S. Francisco, An ab initio study of the competing reaction channels in the reaction of HOCO radicals with NO and O_2, J. Chem. Phys. 120 (2004) 5073–5080.
[63] I. ANSYS, ANSYS Chemkin-Pro Reaction Workbench 2020 R2, 2020.
[64] A.M. Dean, J.E. Hardy, R.K. Lyon, Kinetics and mechanism of NH_3 oxidation, Symp. (Int.) Combust. 19 (1982) 97–105.
[65] S. Kasaoka, E. Sasaoka, M. Nagahiro, K. Kawakami, Non-catalytic reduction of nitrogen monoxide with ammonia and oxidation of ammonia with oxygen, Nippon Kagaku Kaishi (1) (1979) 138–144.
[66] M.U. Alzueta, M. Abián, I. Elvira, V.D. Mercader, L. Sieso, Unraveling the NO reduction mechanisms occurring during the combustion of NH_3/CH_4 mixtures, Combustion and Flame (2022) In press.